Chapter 5

Jatropha curcas oil based alkyd/epoxy/graphene oxide (GO) bionanocomposites: Effect of GO on curing, mechanical, and thermal properties

GRAPHICAL ABSTRACT

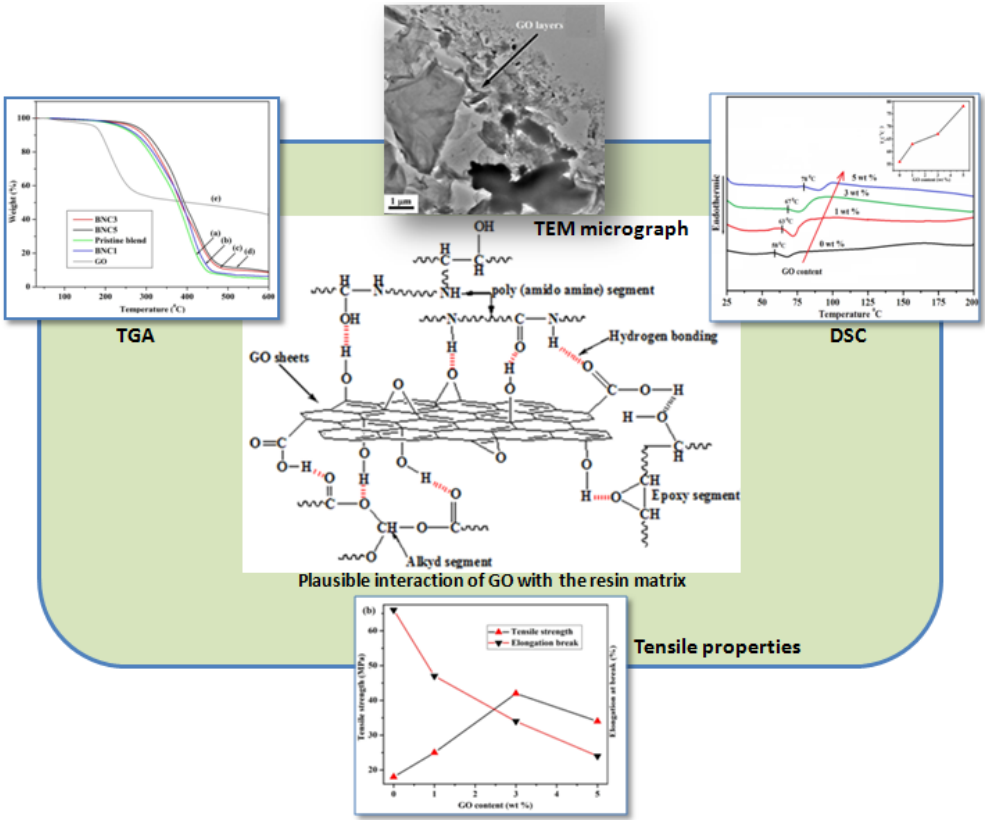

5.1 Introduction

During recent years, increased attention has been devoted to the development of bionanocomposites.[1] Bionanocomposites are a class of materials consisting of a natural polymeric matrix reinforced with organic/inorganic nano fillers. In general, a polymer nanocomposite is a multiphase material which has at least one dimension in the range 1–100 nm or structures that exhibit nanoscale repeat distances between the different phases that make up the material. The bionanocomposite shows the significant advantages of exhibiting biodegradability and biocompatibility in various applications, agricultural, medicinal, drug release, packaging fields.[2,3]

Vegetable oil based alkyd resins have a number of advantages, including versatility in structure and properties, overall low cost, ease of application and are renewable. However, they suffer some major drawbacks such as poor alkali resistance, inferior mechanical properties, low hardness and thermal stability and long curing time as compared to epoxy resins. To improve these drawbacks, alkyd resins are blended with other suitable resins, such as epoxy resin, amino resin, silicone resin and ketonic resin. The thermal and mechanical properties of these polymers can be improved further by the decoration of nanocomposites.[4,5]

Nanocomposites containing multifunctional nano fillers such as graphite, carbon nanotubes (CNT), fullerenes, and silicates are being developed with good mechanical, thermal, and electrical properties.[6-8] In our earlier work we have reported the preparation of *Jatropha curcas* oil based alkyd/epoxy/EG biocomposite with significant improvement

A part of this chapter is published

P. Gogoi, R. Boruah, S.K. Dolui, *Progress in Organic Coatings* 2015, 84, 128–135.

in thermal and mechanical properties.[5] Yasmin et al. studied the structural, mechanical, viscoelastic and thermal properties of graphite platelet/epoxy nanocomposite. The nanocomposite showed good thermal, mechanical, and rheological behaviour.[9] Bharadwaj et al. reported the preparation of unsaturated polyester/organically modified clay nanocomposites, cross-linked with methyl ethyl ketone peroxide (MEKP) with good thermal, mechanical, and rheological properties.[10] Seyhan et al. prepared CNT/polyester nanocomposites using three-roll mill and sonication techniques. The CNT/polyester blend exhibited a shear thinning behavior, while polyester matrix acts as a Newtonian fluid. Nanotubes modified with amine functional groups showed superior tensile strength, as compared to those with untreated CNTs.[11] Battisti et al. investigated the electrical conductivity of unsaturated polyester/multiwalled CNTs nanocomposites. The nanocomposite found to be more conducting with percolation threshold at 0.026 wt % CNTs.[12]

During the last half decade, GO, a two-dimensional single sheet of graphite oxide has attracted a great deal of interest. It is because of its low cost, unique structure, remarkable properties. GO can be prepared in large scale from low cost natural graphite which is an easily available material.[13-15] The presence of oxygen functional groups such as hydroxyl, carboxyl, carbonyl and epoxide facilitate easy dispersion of GO sheets in polar solvents. Moreover, the functional groups in the GO sheets impart strong interaction with polar molecules or polymers to form GO-intercalated or exfoliated composites.[16-18] It offers the possibility of making multifunctional nanocomposites in a cost effective way over other expensive fillers like CNT. There are several reports on GO based polymer nanocomposites with significant improvement in the thermal, mechanical and electrical properties. Wang et al. studied the curing dynamics and network formation of cyanate ester resin/GO nanocomposites. The incorporation of GO into the resin matrix showed a strong catalytic effect on the cure of the resin, and addition of 4 wt % GO resulted in the decrease of curing temperature to 97 °C.[19-21]

Inspiring from those studies, the objective of our present work is to fabricate bionanocomposite films that contain reinforcing GO nanofillers in an alkyd/epoxy blend

matrix and to evaluate mechanical and thermal properties. The structure and property relationship of the bionanocomposites are also investigated. This study aims at obtaining a well dispersion of GO sheets throughout the polymer matrix as well as to accomplish significant improvement in thermal and mechanical properties. The introduction of minute amount of GO greatly enhance the properties of alkyd/epoxy blend matrix.

5.2 Experimental

5.2.1 Materials

Jatropha oil modified alkyd resin with 100% phthalic anhydride was prepared by the method referred in Chapter 2. Epoxy resin (Epoxy equivalent weight: 170-180 g/eq) and hardener poly(amido amine), MEKP and cobalt octoate of commercial grade (Kumud Enterprises, Kharagpur, West Bengal, India) were used as received. Graphite flakes was purchased from Sigma–Aldrich with a particle size of 150 µm and purity of 99.9%. All of the other solvents and materials were of analytical grade, commercially available and used without further purification.

5.2.2 Preparation of graphene oxide (GO)

GO prepared from natural graphite using a modified Hummers method.[22] In a typical method graphite (5 g) and $NaNO_3$ (2.5 g) were mixed with H_2SO_4 (120 mL) in a 500 mL beaker and the mixture was stirred for 30 min in an ice bath. Under vigorous stirring, 15 g of $KMnO_4$ was added to the suspension at a controlled rate to keep the reaction temperature below 20 °C. The mixture was allowed to stir for 12 hrs at room temperature. Afterward 150 mL of distilled water was added slowly to the reaction mixture and allowed to stay for 24 hrs under vigorous stirring. Then 50 mL 30% H_2O_2 was added and stirred for 6 hrs. Finally the mixture was washed with 5% of HCl followed by water until the pH of the filtrate was 7 and dried in a vacuum oven.

5.2.3 Preparation of alkyd/epoxy/GO bionanocomposite

The alkyd/epoxy/GO bionanocomposite was prepared by solution blending method. The alkyd and epoxy was blended at the ratio of 1:1 in acetone (1mg/mL) and then GO

was added in different wt % (Table 5.1). The mixture was stirred by mechanical stirrer followed by ultra-sonication for 1.5 h to get exfoliated and homogeneous dispersion of the GO nano-sheets in the polymer matrix. The solvent was evaporated at 55 °C and the mixture was dried at 40 °C in a vacuum oven until it was completely bubble free. Afterward, poly (amido amine) (50 wt % with respect to the epoxy resin) along with MEKP and cobalt octoate (4 and 2 wt % respectively with respect to the alkyd resin) were added to the mixture. The mixture was then placed on a Teflon sheet by an applicator maintaining the film thickness of 0.3 mm and dried under vacuum in a desicator for overnight at ambient temperature. The bionanocomposite was allowed to cure at 70 °C for further study. The curing time of the bionanocomposites with different wt % GO was recorded.

Table 5.1: Compositions of the bionanocomposites.

entry	sample particulars*	alkyd (g)	epoxy (g)	GO (wt %)
1	BNC0	2	2	0
2	BNC1	2	2	1
3	BNC3	2	2	3
4	BNC5	2	2	5

*In the sample particulars the number denotes the wt % of GO.

5.3 Instruments and methods

5.3.1 Fourier transform infrared spectrometer (FT-IR)

To gain insights into the structural information of prepared hydrogels, the IR spectra of the hydrogels were recorded with a Nicolet Impact-410 IR spectrometer (USA) in KBr medium at room temperature in the region 4000-450 cm^{-1}.

5.3.2 X-ray diffractometer (XRD)

Powder X-Ray diffraction (XRD) data were collected on a Rigaku Miniflex X-ray diffractometer (Tokyo, Japan) with Cu Kα radiation (λ=0.15418 Å) at 30 kV and 15 mA

with a scanning rate of $0.05^{o}s^{-1}$ in a 2θ ranges from 10-70^{o} for the neat alkyd/epoxy blends and the alkyd/epoxy/GO bionanocomposites.

5.3.4 Scanning electron microscope (SEM)

The surface morphology of the specimens was studied by scanning electron microscope (SEM) of model JSM-6390LV, JEOL, Japan at an accelerating voltage of 5-15 kV. The surface of the specimens was coated with platinum before the SEM analysis.

5.3.5 Transmission electron microscope (TEM)

To study the dispersion and delamination of GO sheets, a PHILIPS CM 200 transmission electron microscope (TEM) was used (200 kV).

5.3.6 Thermogravimetric analysis (TGA)

To study the thermal degradation of the bionanocomposites, thermogravimetric analysis (TGA) was carried out on a Shimazdu TGA 50, thermal analyzer in nitrogen atmosphere at a heating rate of 10 °C min^{-1} in the temperature range 25-600 °C.

5.3.7 Differential scanning calorimetry (DSC)

The glass-transition and crystallization behaviors were investigated by differential scanning calorimetry using a Shimadzu DSC-60 in nitrogen atmosphere. The analysis was run at a scanning speed of 10 °C min-1 from 25-250 °C.

5.3.8 Mechanical property

The tensile strength, elongation, and elastic modulus of the bionanocomposites were measured on a universal tensile testing machine (Zwick Z010, Germany) at ambient conditions. The extension rate was 5 mm/min and the load cell was 10-kN, with a gauge length of 40 mm. The specimen dimension was 60 mm in length, 10 mm in width, and 0.3 mm in thickness. Three parallel measurements were carried out for each sample.

5.3.9 Viscosity measurement

The viscosity of the composites under a constant shear stress of 100 Pa is measured by a modular compact rheometer (MCR 500, Physica, Anton Paar) at 25 ºC.

5.4 Results and discussion

Alkyd/epoxy/GO bionanocomposite films were prepared by dispersing different concentrations of GO in alkyd/epoxy resin blend matrix and subsequently cross-linked. The bionanocomposite film is highly flexible and shown in Fig. 5.1.

Fig. 5.1: Photograph of a alkyd/epoxy/GO bionanocomposite film.

5.4.1 Rheological and curing study of the bionanocomposites

It is observed that the viscosity of the alkyd/epoxy/GO bionanocomposites increases gradually with increasing GO concentration (Table 5.2). The viscosity of the alkyd/epoxy blend is found to be 5.75 Pa.s. However, the viscosity of alkyd/epoxy/GO bionanocomposites with 1, 3, and 5 wt % GO is increased to 6.42, 6.97, and 7.63 Pa.s respectively. It is obvious that incorporation of GO decreases the fluidity of the composites by the strong interaction (H-bonding and/or dipolar) with the polymer matrix (Scheme 5.1).

Table 5.2: Viscosity and curing characteristics of the bionanocomposites.

GO content (wt %)	viscosity (Pa.s)	curing time (min)	curing temperature (°C)
0	5.75	75 ± 2	70
1	6.42	71 ± 2	70
3	6.97	63 ± 2	70
5	7.63	57 ± 3	70

*viscosity of the composites is measured before curing.

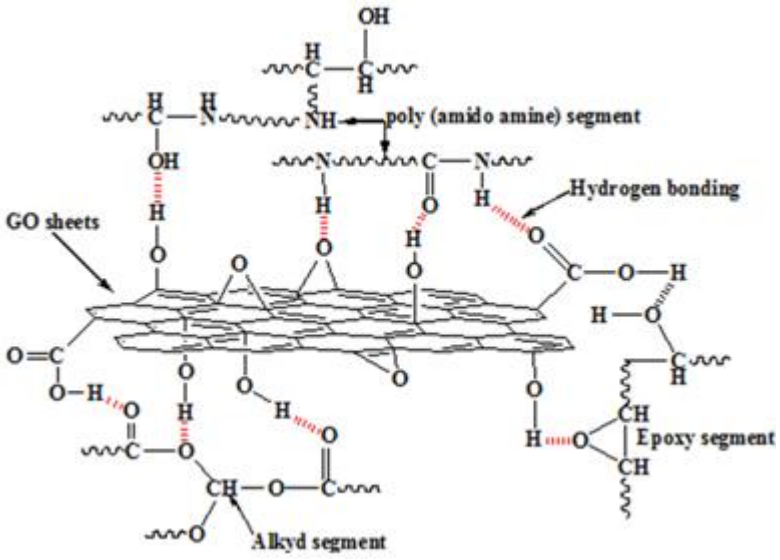

Scheme 5.1: Proposed possible interactions of GO with the polymer matrix.

The curing characteristics of the bionanocomposites are summarized in Table 5.2. It is observed that the curing time decreases gradually with increasing GO concentration. The decrease in curing time by the presence of GO can be explained using Arrhenius theory, which is referred to that the reaction rate constant is dependent on reaction temperature, collision factors as well as the activation energy. In relation to this investigation, it is assumed that when the GO is incorporated into the polymer matrix the diffusion of the reactive species for cross-linking will be restricted due to filler-filler interaction in the GO sheets. This implies that the GO caused an increase in the collision factor of the reactive species around the neighbourhoods in the cross-linking system.

Therefore, this resulted in an auto-acceleration reaction of the alkyd/epoxy/GO bionanocomposite system.[20,23]

5.4.2 FT-IR analysis

In the FT-IR spectrum of GO (Fig. 5.2b)], the broad peak at 3423 and peak at 1629 cm^{-1} can be attributed to -OH stretching and C=O stretching respectively,[24] which can facilitate the physical and chemical interactions with the functionalities of the polymer matrix.[25] The peaks at 1185 and 1091 cm^{-1} are assigned to ring stretching and the peak at about 640 cm^{-1} is assigned to symmetric ring deformation of epoxy group present in the GO sheets. As -OH stretching and C-OH stretching peaks are sensitive to hydrogen bond, shifting of peak at 3413 and 1729 cm^{-1} to lower wave number in the bionanocomposites (Fig. 5.2c) indicates the interactions of the GO nano-sheets with the alkyd/epoxy blend matrix through hydrogen bonding or other polar-polar interactions (Scheme 5.1).[26] Another similar change in the FT-IR spectrum of the alkyd/epoxy/GO bionanocomposite is also observed for the peak corresponding to the C-OH stretching at about 1170 cm^{-1}, indicating hydrogen bonding between the -OH groups in GO nano-sheets and the oxygenated groups in alkyd/epoxy blend (Scheme 5.1).[27] However, the disappearance of

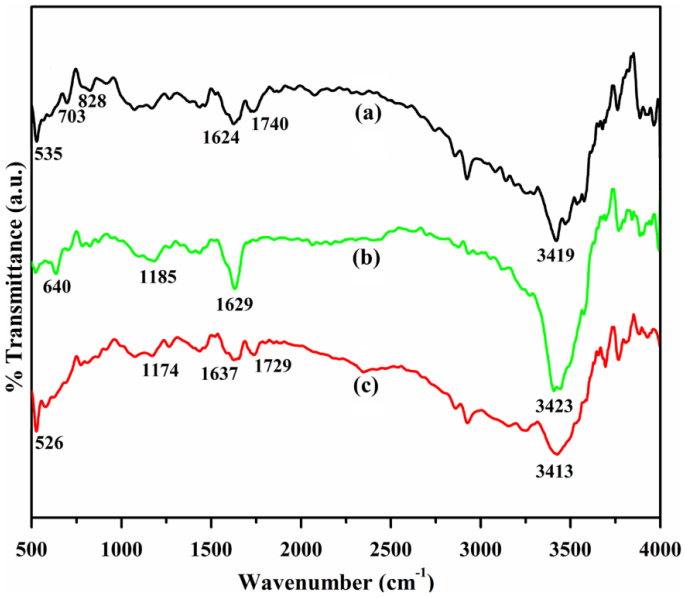

Fig. 5.2: FT-IR spectra of (a) alkyd/epoxy blend, (b) GO and (c) bionanocomposite (3 wt % GO).

the peak at 703 cm^{-1} is assigned to out-of-plane vibration of the -OH group, while the peak at 828 cm^{-1}corresponds to the out-of-plane vibration of the C-H group. The disappearance of these peaks in the bionanocomposite suggests that interaction between GO nano filler and the polymer matrix takes place over -OH group. It also appears that the attachment of GO nano fillers to the polymer chains prevents the out-of-plane oscillations of C-H group.[28] Thus, FT-IR study reveals that GO has been successfully incorporated in the polymer matrix.

5.4.3 X-ray diffraction (XRD) analysis

The structure and apparent interlayer spacing (d spacing) of the alkyd/epoxy/GO bionanocomposites prepared via solution intercalation have been detected by XRD. Fig. 5.3 shows the XRD patterns for the GO, pristine polymer and the bionanocomposites. The basal spacing of GO has been calculated to be 0.786 nm from a diffraction peak at 2Θ = 11.3° using Bragg function. The pristine polymer shows no diffraction peak in the 2Θ range from 2 to 15° showing that the alkyd/epoxy blend has no ordered structure in this dimension range but exhibits a weak and a broad diffraction peak at 20.45° which indicates that the alkyd/epoxy resin blend is amorphous in nature. The diffraction peak of

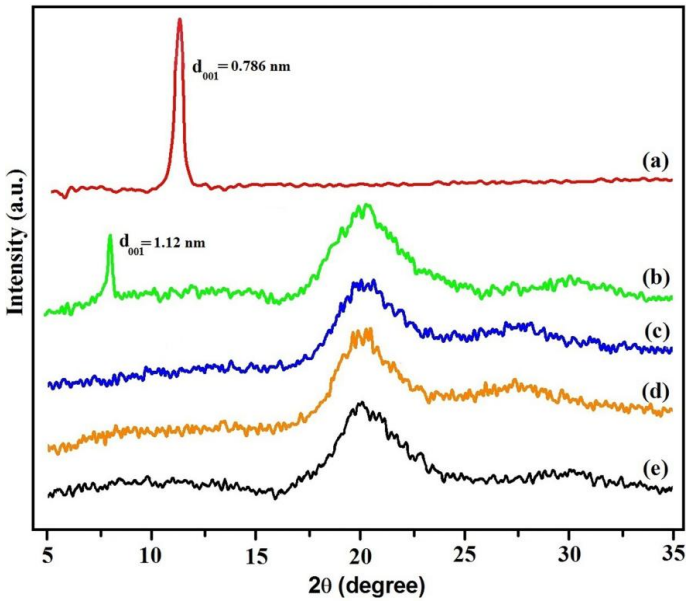

Fig. 5.3: XRD patterns of (a) GO, (b) BNC5, (c) BNC3, (d) BNC1 and (e) pristine blend.

the GO was absent in the X-ray diffractrograms for the 1 wt % and 3 wt % GO loaded bionanocomposites (Fig. 5.3c & d). It clearly demonstrates the disappearance of the regular and periodic structure of GO and the formation of fully exfoliated structures and the homogeneous distribution of GO nano-sheets in the polymer matrix.[21,29] From the Fig. 5.3 it is clear that the peak obtained for GO at around $2\Theta = 11.3°$ is shifted towards lower diffraction angle ($2\Theta = 7.9°$) with the reduction in intensity in 5 wt % GO loaded bionanocomposites (Fig. 3b). This indicates that the layers in GO was delaminated during the mixing process by the polymer chains and forms an intercalated structure.[30,31]

5.4.4 Morphological studies

The microstructure of alkyd/epoxy/GO bionanocomposites has been visualized by using TEM, as TEM studies are necessary to verify the extent of delamination and exfoliation achieved and the images are shown in Fig. 5.4.[31] It is observed that in the bionanocomposite, GO layers are well dispersed. In this case, both XRD and TEM confirm that a highly exfoliated alkyd/epoxy/GO bionanocomposite has been achieved. A very similar result was observed with sodium carboxymethyl cellulose/GO nanocomposites.[32] Although the GO lattices still retain their orientation to some degree, the GO layers are highly exfoliated into some thin sheets by the polymer matrix with a dimension of about 10-15 nm in thickness. When the GO content is 5 wt % the layered structure of the GO is generally intercalated in the polymer matrix (Fig. 5.4d). The d-spacing value increases from 0.786 nm for the pristine GO to 1.12 nm, which is in good agreement with the results from the XRD experiments. Similar results were observed for the poly(vinyl acetate)/graphite oxide nanocomposites.[14] On the basis of the evidence from XRD and TEM, the alkyd/epoxy/GO bionanocomposites with a highly exfoliated or intercalated structure have been prepared via solution blending method with the aid of ultra-sonication followed by mechanical stirring (Scheme 5.2). The results obviously suggest a high affinity between alkyd/epoxy blend matrix and GO. This should be assigned to some kind of interactions, such as hydrogen bonding and/or electrostatic interaction.[30]

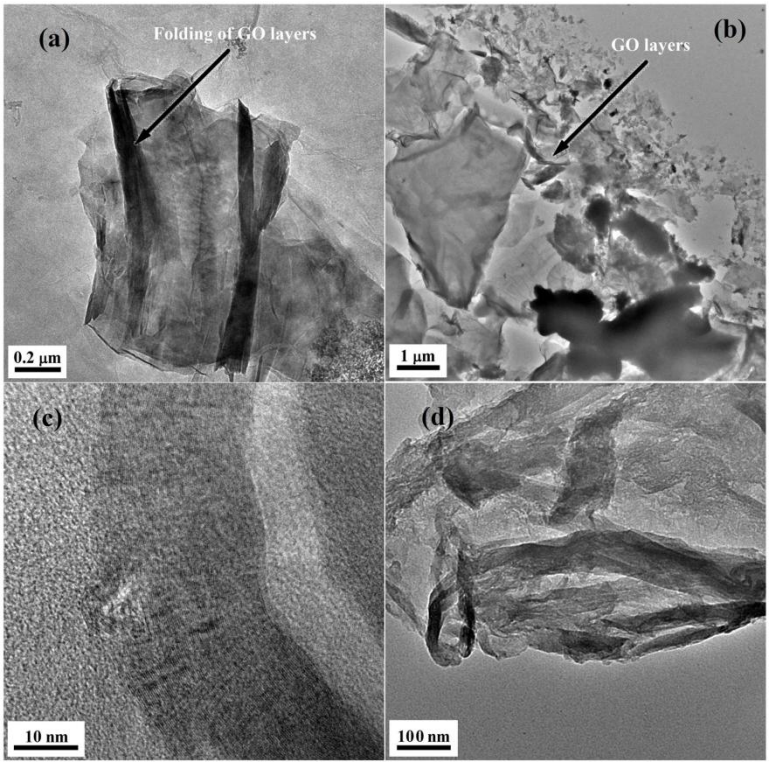

Fig. 5.4: TEM micrographs of the bionanocomposites at different magnifications, (a) 1 wt %, (b) & (c) 3 wt % and (d) 5 wt % GO.

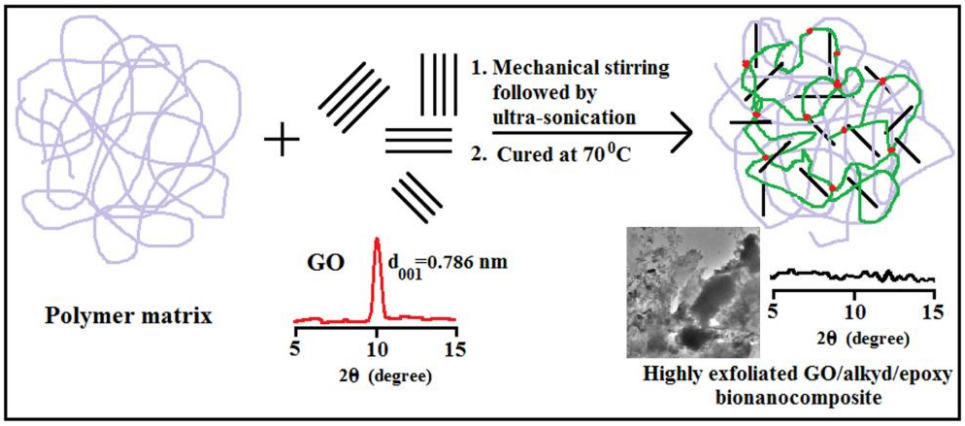

Scheme 5.2: Schematic representation of the formation of highly exfoliated GO/alkyd/epoxy bionanocomposite.

The interfacial interactions between the polymer matrix and GO nano-sheets are further investigated by the SEM study of the fracture surfaces as shown in Fig. 5.5. The SEM image of the pristine polymer is characterized with smooth surface (Fig. 5a).

However, the fracture surfaces of the alkyd/epoxy/GO bionanocomposite films after tensile testing are totally different from that of the pristine polymer (Fig. 5b & c), in which the surface is affected by the exfoliation of GO sheets. These are also different from the films of the polymer/carbon nanotubes composites.[33] It is characterized by the hybrid structure of the bionanocomposites which appears gradually as separated parallel layers with the addition of GO nano filler, just like that of the GO membrane.[34] It suggests that the acetone-dispersed GO and alkyd/epoxy blend matrix accumulate into a layer-stacking micro-structure. Similar results were observed for poly(vinyl alcohol)/GO nanocomposites.[21]

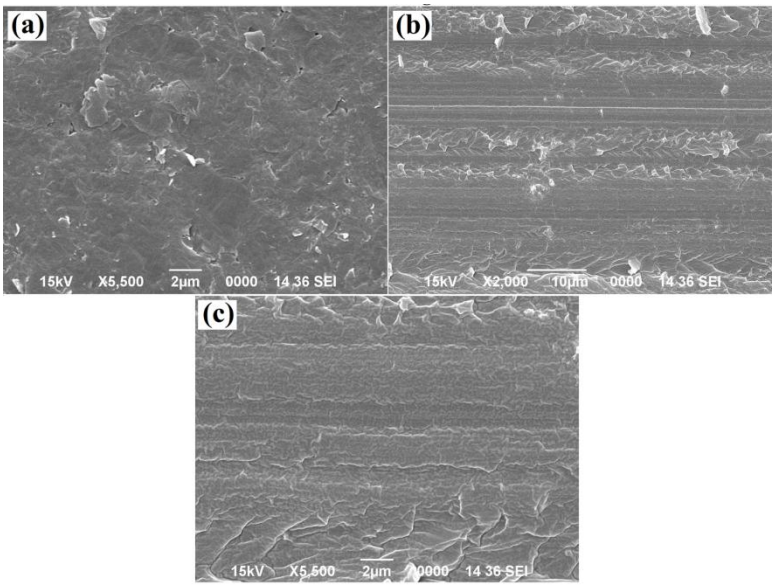

Fig. 5.5: SEM images of the fracture surface of (a) alkyd/epoxy blend and (b) & (c) BNC3.

5.4.5 Thermal characterization of the bionanocomposites

5.4.5.1 DSC study

The glass transition behavior of the pristine polymer and the bionanocomposites are investigated by differential scanning calorimetry and the curves are shown in Fig. 5.6. The glass transition temperature (T_g) of the alkyd/epoxy blend increases significantly from 58 to 78 °C with 5 wt % GO. It is also observed that the T_g increases by 5 and 9 °C as compared to the pristine polymer when GO content is 1 and 3 wt % respectively. The

increase in T_g can be explained by reduced mobility of the polymer chains attached to the surface of the GO sheets by hydrogen bonding and/or electrostatic interaction.[21] Moreover, the fine dispersion of GO sheets effectively restricts the segmental motion of the polymer chains on the interface of the GO layers because of their high aspect ratio and reactive surface.[30] The results clearly indicate the strong interaction between the alkyd/epoxy blend matrix with the GO sheets which is also supported by FT-IR study.

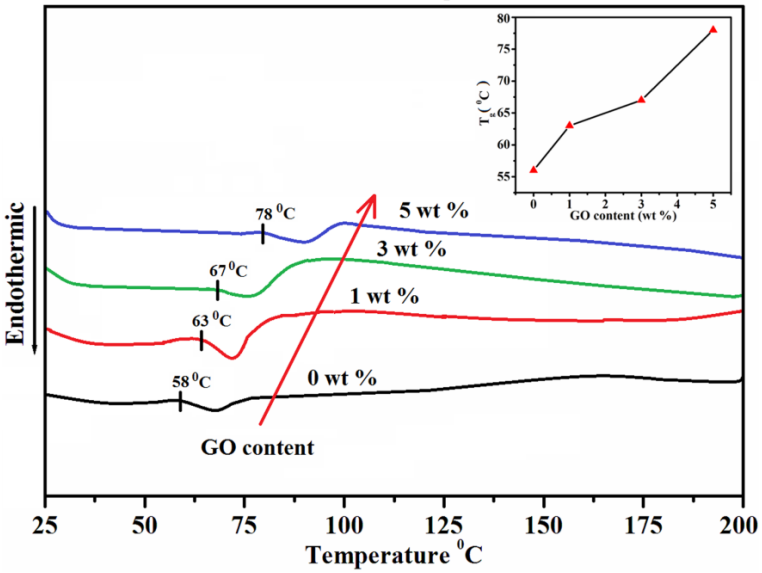

Fig. 5.6: DSC traces of the pristine blend and the bionanocomposites. Inset is the T_g vs GO content (wt %).

5.4.5.2 Thermogravimetric analysis

Thermal property represents one of the most important properties in polymer nanocomposites. Thus, the thermal stability of the alkyd/epoxy/GO bionanocomposites was investigated by using TGA and the weight loss traces recorded in the temperature range 25-600 °C. Fig. 5.7 presents the TGA thermograms of GO, pristine polymer and the alkyd/epoxy/GO (1-5 wt %) bionanocomposites and the data are summarized in Table 5.3. The initial 4% weight loss of GO (Fig. 5.7e) at around 100 ºC can be attributed to the removal of water molecules trapped inside the GO structure. The rapid weight loss of 37% at around 200-240 ºC is assigned to the pyrolysis of the labile oxygen containing functional groups in the forms of CO, CO_2 and steam.[35] It is observed that GO and

alkyd/epoxy blend matrix has synergistic effect on the thermal stability of alkyd/epoxy/GO nanocomposites, i.e. the bionanocomposites has much improved thermal stability than the individual components. Furthermore the thermal stability of the alkyd/epoxy/GO bionanocomposites increases gradually with increasing GO content. For example, the major degradation step is shifted to higher temperature by about 29 °C and 39 °C for the nanocomposites with 3 and 5 wt % GO. In all the cases, the thermal degradation occurs in one step, which is mainly due to the degradation of cross-linked polymer network. The degradation of polymers starts with the free radical formation at the weak bonds and/or chains ends, followed by radical transfer to adjacent chains via inter chain reactions. The improved thermal stability can be explained through the reduced mobility of the polymer chains in the bionanocomposite. As a result of the reduced chain mobility the chain transfer reaction will be suppressed and consequently the degradation process will be slowed and decomposition will take place at higher temperature.[28] The observed behavior is most likely the consequence of the homogeneous dispersion and strong interfacial interaction between the GO nano filler and the polymer matrix. Moreover, the incorporation of GO within the polymer matrix acts as a mass transport

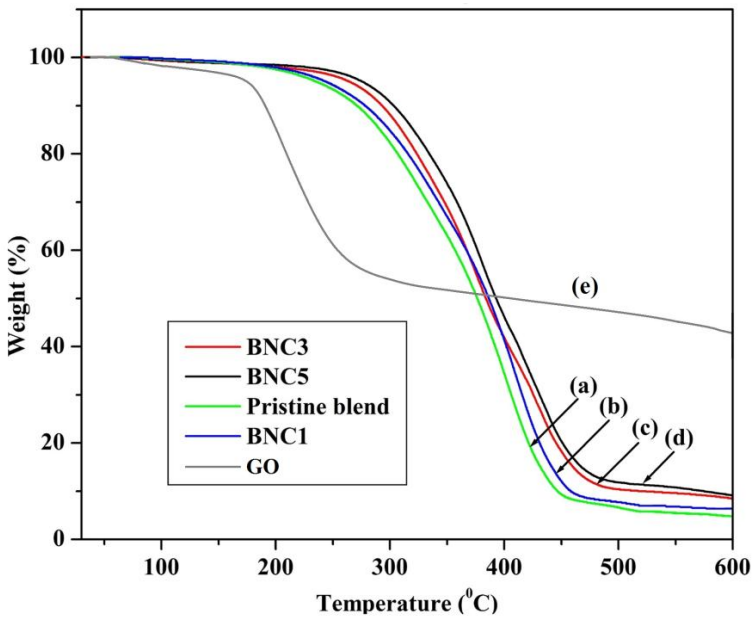

Fig. 5.7: TGA curves of (a) pristine blend, (b) BNC1, (c) BNC3, (d) BNC5, and (e) GO.

barrier to the volatile products generated during degradation process and increases the overall thermal stability of the bionanocomposites.[5] Higher the amount of GO in the composites more pronounced is the effect. The improvement of thermal stability of alkyd/epoxy/GO bionanocomposites is very similar with other polymer/GO nanocomposites.[32] The bionanocomposites shows higher char content at 600 °C as the wt % of GO increases (Table 5.3). It is probably due to the formation of carbon net structure (graphene and/or expanded graphite) in the composites.[36] The char content is about 6, 8 and 9.5% for bionanocomposites with 1, 3 and 5 wt % GO respectively, whereas the same about 5% for the pristine polymer.

Table 5.3: TGA data of the pristine blend and the bionanocomposites.

GO content (wt %)	major degradation temperature, T_d (°C)	weight loss (%) at temperature (°C)				char (%) at 600 °C
		200	300	400	500	
0	251	2.6	18	67	93	5 ± 1
1	262	2.2	15	60	91	6 ± 2
3	280	1.7	12	58	88	8 ± 2
5	290	1.4	9	54	86	9 ± 3

5.4.6 Mechanical properties

GO nano fillers is expected to have good reinforcement effect for tensile properties due to its large aspect ratio and excellent mechanical strength.[37] The tensile strength of alkyd/epoxy/GO bionanocomposites increases significantly as compared with that of the pristine polymer matrix (Table 5.4).

The effect of GO content on the elastic modulus of the composite films is shown in Fig. 5.8(a). The elastic modulus of the composite films increases from 1.27 to 2.14 and 2.42 GPa with 3 and 5 wt % GO respectively. It is noticeable that bionanocomposite reinforced with only 1 wt % GO showed about 44% increase in elastic modulus over the pristine polymer matrix. As a result of the strong attachment of polymer chain segments

with the GO sheets, the transfer of mechanical energy from the matrix to high strength filler increases significantly, i.e., the elastic modulus of the material as a whole increases. However, the variations in tensile strength with GO content do not follow the same trend (Fig. 5.8(b)). The tensile strength of the bionanocomposite is 42 MPa with 3 wt % GO loading. Whereas, the tensile strength decreased to 34 MPa with 5 wt % GO. It can be assumed that at higher GO content, particle aggregation is taking place.[9] The improvement in tensile strength and elastic modulus results from the high strength and high aspect ratio of GO nano filler as well as homogeneous dispersion and good interfacial interaction between the GO sheets and the alkyd/epoxy blend matrix. However, the lower strength at higher GO content (5 wt %) can be attributed to the aggregation of nano fillers in the bionanocomposite film. The TEM micrographs of the bionanocomposite with 5 wt % GO loading (Fig. 4(d)) also confirms this.[29]

From the Fig. 5.8(b) it is clear that the elongation at break of the bionanocomposite films gradually decreases with increasing GO loading. The average values of elongation at break decreased to 24% for the bionanocomposite reinforced with 5 wt % GO. Whereas, the pristine polymer showed elongation at break about 66%. Similar results were perceived for other graphene/GO-based polymer composites.[38,39] The reason can be ascribed to the high aspect ratio of GO nano filler as well as strong interaction between both the components which reduces the polymer chain mobility.[5]

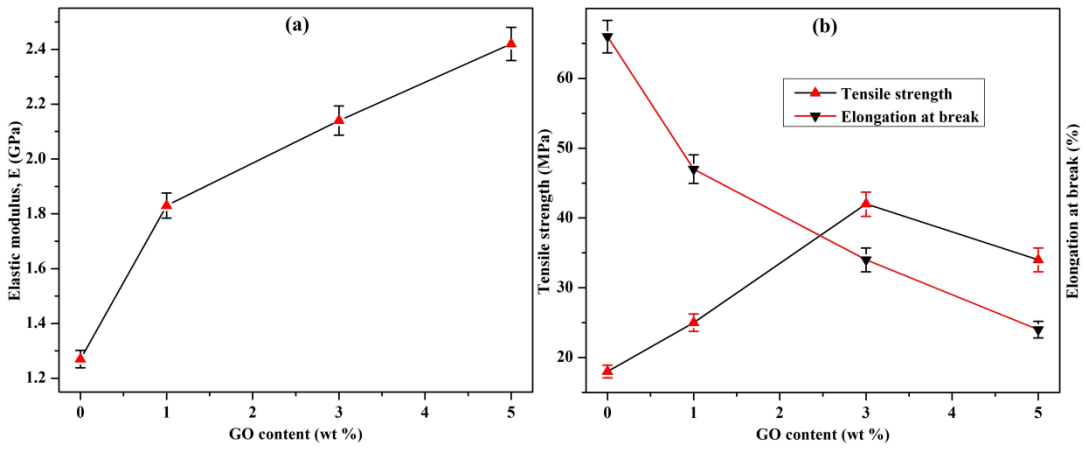

Fig. 5.8: Effect of GO content on the mechanical properties of the bionanocomposites, (a) elastic modulus, and (b) tensile strength.

Table 5.4: Mechanical properties of the bionanocomposites.

GO content (wt %)	tensile strength (MPa)	elastic modulus, E (Gpa)	elongation at break (%)
0	18 ± 2	1.27 ± 0.2	66 ± 3
1	25 ± 4	1.83 ± 0.2	47 ± 5
3	42 ± 3	2.14 ± 0.1	34 ± 3
5	34 ± 3	2.42 ± 0.1	24 ± 4

5.5 Conclusion

- Jatropha oil modified alkyd resins and GO based bionanocomposites were prepared successfully by solution intercalation method.
- GO significantly accelerates the curing rate of the alkyd/epoxy blends.
- XRD and TEM study revealed the formation of highly exfoliated structures and the homogeneous distribution of GO nano-sheets within the polymer matrix.
- Homogeneous dispersion and strong interfacial adhesion of GO with the polymer matrix significantly improved the thermo-mechanical properties of the bionanocomposites.
- The thermal stability of the bionanocomposites increased upto 39 °C by the incorporation of GO.
- The tensile strength and elastic modulus of the alkyd/epoxy/GO bionanocomposites increased by 133% and 68%, respectively.
- The results of the study showed that the bionanocomposite with 3 wt % GO showed the best balance of thermal and mechanical properties.

References

1. Tingaut, P., et al. *Biomacromolecules* **11** (2), 454-464, 2010.
2. Habibi, Y., et al. *J. Mater. Chem.* **18** (41), 5002-5010, 2008.
3. Mangiacapra, P., et al. *Carbohyd. Polym.* **64** (4), 516-523, 2006.
4. Chivrac, F., et al. *Mater. Sci. Eng. R.* **67** (1), 1-17, 2009.
5. Gogoi, P., et al. *Prog. Org. Coat.* **77** (1), 87-93, 2014.
6. Aziz, S.H., et al. *Compos. Sci. Technol.* **65** (3-4), 525-535, 2005.
7. Battisti, A., et al. *Compos. Sci. Technol.* **69** (10), 1516-1520, 2009.
8. Tibiletti, L., et al. *J. Polym. Degrad. Stab.* **96** (1), 67-75, 2011.
9. Yasmin, A., & Daniel, I.M. *Polymer* **45** (24), 8211-8219, 2004.
10. Bharadwaj, R.K., et al. *Polymer* **43** (13), 3699-3705, 2002.
11. Seyhan, T., et al. *Eur. Polym. J.* **43** (2), 374-379, 2007.
12. Battisti, A., et al. *Compos. Sci. Technol.* **70** (4), 633-637, 2010.
13. Han, Y., & Lu, Y. *Comp. Sci. Technol.* **69** (7-8), 1231-1237, 2009.
14. Liu, P.G., et al. *J. Mater. Chem.* **10** (4), 933-935, 2000.
15. Xu, J., et al. *Carbon* **40** (3), 450-451, 2002.
16. Verdejo, R., et al. *J. Mater. Chem.* **18** (19), 2221-2226, 2008.
17. Du, X., et al. *Chem. Mater.* **20** (6), 2066-2068, 2008.
18. Yang, Y., et al. *Langmuir* **25** (19), 11808-11814, 2009.
19. Chen, Y., et al. *Eur. Polym. J.* **48** (6), 1026-1033, 2012.
20. Wang, X., et al. *Eur. Polym. J.* **48** (6), 1034-1041, 2012.
21. Yang, X., et al. *J. Appl. Polym. Sci.* **120** (3), 1355-1360, 2011.
22. Hummers, W.S., & Offeman, R.E. *J. Am. Chem. Soc.* **80** (6), 1339-1339, 1958.
23. Sriloy, N., et al. *Macromol. Res.* **18** (4), 372-379, 2010.
24. Wang, H., et al. *Appl. Mater. Interfaces* **2** (3), 821-828, 2010.
25. Dhakate, S.R., et al. *Int. J. Hydrogen Energ.* **33** (23), 7146-7151, 2008.
26. Lu, L.Y., et al. *J. Membr. Sci.* **281** (1), 245-252, 2006.
27. Matsuo, Y., et al. *Chem. Mater.* **10** (8), 2266-2269, 1998.
28. Mbhele, Z.H., et al. *Chem. Mater.* **15** (26), 5019-5024, 2003.
29. Du, X.S., et al. *Carbon* **43** (1), 195-197, 2005.

30. Chen, P., & Zhang, L. *Biomacromolecules* **7** (6), 1700-1706, 2006.

31. Yoonessi, M., et al. *Macromolecules* **37** (7), 2511-2518, 2004.

32. Layek, R.K., et al. *Macromol. Mater. Eng.* **298** (11), 1166-1175, 2013.

33. Wang, S.F., et al. *Biomacromolecules* **6** (6), 3067-3072, 2005.

34. Chen, C., et al. *Adv. Mater.* **21** (29), 3007-3011, 2009.

35. Zhang, Y., et al. *J. Mater. Chem.* **22** (26), 13064-13069, 2012.

36. Konwer, S., et al. *J. Electron Mater.* **40** (11), 2248-2255, 2011.

37. Wang, G., et al. *Carbon* **47** (14), 3242-3246, 2009.

38. Xu, Y., et al. *Carbon* **47** (15), 3538-3543, 2009.

39. Zhao, X., et al. *Macromolecules* **43** (5), 2357-2363, 2010.